Print ISSN : 0022-2755
Journal of Mines, Metals and Fuels
Contents available at: www.informaticsjournals.com/index.php/jmmf

Two Component Benard-Marangoni Convection in A Composite System Subjected to Variable Heat Source

Sumithra. R[1], Archana. M. A.[2*] and Deepa. R. Acharya[3]

Department of UG, PG Studies and Research in Mathematics, Government Science College Autonomous, Bengaluru, Karnataka, India. e-mail: sumitra diya@yahoo.com / archanamurthy78@gmail.com / deeparacharya24@gmail.com

Abstract

Double diffusive convection is the phenomena that describes the convection driven by two differ- ent densities which have different rates of diffusion. A comparison of two temperature boundaries when i) both the surfaces are set at adiabatic temperature, and ii)upper free surface is adiabatic and lower rigid surface is isothermal cases, on surface tension driven double diffusive convection in a horizontal composite layer is studied analytically using exact method. For both cases i) and ii), the thermal Marangoni number (Tmn) is determined, which is the eigen value, for upper free and lower rigid velocity boundary conditions. The results indicate that the given system is a fluid dominant composite system and adiabatic-isothermal thermal boundary is more stable compare to adiabatic-adiabatic boundary condition.

Keywords: *Marangoni convection, Double diffusive convection, variable heat source.*

1. Introduction

Marangoni convection is the mass transfer along an interface between two fluids due to surface tension gradients. Bergman (1986) demonstrated that surface tension in a binary fluid fluctuates with temperature and species concentration if both contribute oppositely at a free surface. In the science of convection, the study of convective motions when there are many diffusing components with differing molecular diffusivities is of recent development. In composite layers, double diffusive or two-component convection has a wide range of applications in crsytal growth, solidification of alloys, upwelling of nutrients, controlling the climate of earth, vertical transport of heat and salt in Oceans, astrophysics, geophysics, biology and limnology. A linear stability analysis has been investigated by Ming-Ichar and Ko-TaChaing (1996) in a double diffusive layer. Sumithra (2012) has inves-tigated the onset of double diffusive convection in a two-layer system with a magnetic field for the Darcy-Binnkman model. Recently, Gangadharaiah (2021) has studied double diffusive Marangoni convection in a superposed fluid and saturated anisotropic porous layer.

Hill (2005) studied linear and nonlinear stability analysis at the initiation of double-diffusion con-vection in a fluid-saturated porous layer with a concentration-based internal heat source. Gaikwad and Dhanraj (2014) conducted an analytical study of the effect of an internal heat source on the beginning of both stationary and oscillatory double diffusive convection considering anisotropic porous layer, and also by Altawallbeh et al. (2013) with soret effect. Deepika et al.(2016) investigated the onset of double diffusive natural convection in a fluid saturated porous medium considering temperature and concentration gradients across the surfaces into account. The combined effect of buoyancy and surface tension in a

*Corresponding author

liquid saturated porous layer with temperature and concentration dependent viscosity has been studied by Bahadori and Rezvantalab (2014). Khalid et al. (2016) examined the reaction of Soret and Dufour coefficients in a rotating nanofluid layer with uniform internal heat source and feedback controller on double diffusive convection for rigid-rigid, rigd-free and free-free boundary conditions. Sumithra et al. (2012), (2018), (2020), (2021) investigated the effects linear and non-linear temperature profiles on two-component Marangoni convection composite medium for Darcy and Darcy-Brinkman model, and has extended the same work considering uniform and variable heat source. Most of the researchers have considered double diffusive convection in a single layer with uniform heat source. There are only few works are available on double diffusive surface tension driven convection in a composite layer. In this research paper, we compare two thermal boundaries (i)when both surfaces have symmetric (adiabatic) conditions, and (ii)upper surface of the fluid medium is adiabatic, lower surface of the porous medium is isothermal, on the double diffusive Marangoni convection in a composite layer considering variable heat sources.

2. Mathematical Analysis

We consider an infinite horizontal fluid saturated porous layer of thickness d_m beneath a layer of the same fluid of thickness d. The porous layer's bottom surface is rigid, while the fluid layer's upper surface is free. The thermal boundaries of the composite system are considered for two cases (i) both are adiabatic, (ii) upper layer is adiabatic and lower layer is isothermal. A cartesian coordinate system (x, y, z) is chosen such that the origin is at the interface between the fluid and fluid-saturated porous layer and the z-axis pointing vertically upwards.

The basic governing equations for the above configuration are:

(Subscripts 'f ' and 'm' represents fluid and porous layers respectively) In the fluid layer ($0 \le z \le d$)

$$\nabla \cdot \vec{V_f} = 0 \tag{1}$$

$$\rho_0 \left[\frac{\partial \vec{V_f}}{\partial t} + (\vec{V_f} \cdot \nabla)\vec{V_f} \right] = -\nabla P + \mu \nabla^2 \vec{V_f} \tag{2}$$

$$\frac{\partial T}{\partial t} + (\vec{V_f} \cdot \nabla) T = \kappa \nabla^2 T + Q(T - T_0) \tag{3}$$

$$\frac{\partial c_f}{\partial t} + \left(\vec{V_f} \cdot \nabla\right) c_f = \kappa_{cf} \nabla^2 c_f \tag{4}$$

In the porous medium ($-d_m \le z_m \le 0$)

$$\nabla_m \cdot \vec{V_m} = 0 \tag{5}$$

$$\frac{\rho_o}{\phi} \frac{\partial \vec{V_m}}{\partial t_m} = -\nabla_m P_m - \frac{\mu}{K} \nabla_m \vec{V_m} \tag{6}$$

$$A \frac{\partial T_m}{\partial t_m} + (\vec{V_m} \cdot \nabla_m) T_m = \kappa_m \nabla_m^2 T_m + Q_m (T_m - T_0) \tag{7}$$

$$\phi \frac{\partial c_m}{\partial t_m} + \left(\vec{V_m} \cdot \nabla_m\right) c_m = \kappa_{cm} \nabla_m^2 c_m \tag{8}$$

where $\vec{V_f}$ and $\vec{V_m}$ respectively are the velocity vectors of the fluid in the fluid and porous layers, ρ_0 is the fluid density, μ represents the viscosity of the fluid, P, the pressure, ϕ refers to the porosity, K represents the permeability, $A = \frac{(\rho_0 C_p)_m}{(\rho_0 C_p)_f}$ represents the ratio of heat capacities with C_p as the specific heat, κ and κ_m refers to thermal diffusivities of the fluid and porous layer respectively, T and T_m are the temperatures in the fluid and porous layers, Q and Q_m denotes heat sources in the fluid and porous layers, t denotes time, c and c_m denotes concentrations in the fluid and porous region, κ_{cf} and κ_{cm} denotes solute difffusivities in the fluid and porous medium respectively.

The governing equations are solved assuming the basic state is quiescent [Sumithra et al. (2020)]. The temperature and concentration distributions [see Manjunatha and Sumithra (2018)] are:

$$T_b(z) = \frac{T_u - T_o}{\sin\left(\sqrt{\frac{Q}{\kappa}} d\right)} \sin\left(\sqrt{\frac{Q}{\kappa}} z\right) + T_o, \quad 0 \le z \le d \qquad \text{...(9)}$$

$$T_{mb}(z_m) = \frac{T_o - T_L}{\sin\left(\sqrt{\frac{Q_m}{\kappa_m}} d_m\right)} \sin\left(\sqrt{\frac{Q_m}{\kappa_m}} z_m\right) + T_o, \quad -d_m \le z_m \le 0 \qquad \text{...(10)}$$

$$c_b(z) = c_0 + \frac{(c_u - c_0) z}{d}, \quad 0 \le z \le d \qquad \text{...(11)}$$

$$c_{bm}(z_m) = c_0 + \frac{(c_0 - c_L)}{d_m}, \quad -d_m \le z_m \le 0 \qquad \text{...12)}$$

where $\frac{T_u \sqrt{Q\kappa} \sin\left(\sqrt{\frac{Q_m}{\kappa_m}} d_m\right) + T_L \sqrt{Q_m \kappa_m} \sin\left(\sqrt{\frac{Q}{\kappa}} d\right)}{\sqrt{Q_m \kappa_m} sin\left(\sqrt{\frac{Q}{\kappa}} d\right) + \sqrt{Q\kappa} sin\left(\sqrt{\frac{Q_m}{\kappa_m}} d_m\right)}$ and $c_0 = \frac{c_u d_m \kappa_{cf} + d c_L \kappa_{cm}}{d_m \kappa_{cf} + c_L \kappa_{cm}}$ are the interface temperature and species concentration respectively. T_u represents upper temperature and T_L represents lower temperature, subscript 'b' represents basic state.

Following Sumithra and Manjunatha (2018) the method of infinitesimal pertubations are superim- posed and the governing equations are nondimensionalized by choosing suitable scaling parameters after linearization (see Manjunatha and Sumithra (2018)). The time derivative can be removed from the perturbed dimensionless equations since the concept of exchange of stability holds for the provided composite system. Then we perform normal mode expansion to obtain solutions for w, w_m, θ, θ_m, s, and s_m in the form

$$[w,\theta,s]=[W(z),\Theta(z),S(z)]e^{i(lx+my)} \quad \text{... (13)}$$

$$[w_m,\theta_m,s_m]=[W_m(z_m),\Theta_m(z_m),S_m(z_m)]e^{i(\acute{l}x+\acute{m}y)} \quad \text{... (14)}$$

The differential equations so obtained by applying equations (13) and (14) to the perturbed dimensionless equations are:

$$\left(D^2-a^2\right)^2 W(z)=0 \quad \text{... (15)}$$

$$\left(D_m^2-a_m^2\right)W_m(z_m)=0 \quad \text{... (16)}$$

$$\left(D^2-a^2+R_I\right)\Theta(z)+\frac{W(z)\sqrt{R_I}}{sin\sqrt{R_I}}cos\left(\sqrt{R_I}z\right)=0 \quad \text{... (17)}$$

$$\left(D_m^2-a_m^2+R_{I_m}\right)\Theta_m\left(z_m\right)+\frac{W_m\sqrt{R_{I_m}}}{\sin\sqrt{R_{I_m}}}\cos\left(\sqrt{R_{I_m}}z_m\right)=0 \quad \text{... (18)}$$

$$\tau_f\left(D^2-a^2\right)S(z)+W(z)=0 \quad \text{... (19)}$$

$$\tau_{mp}\left(D_m^2-a_m^2\right)S_m(z_m)+W_m(z_m)=0 \quad \text{... (20)}$$

where $a=\sqrt{l^2+m^2}$ and $a_m=\sqrt{\acute{l}^2+\acute{m}^2}$ are horizontal wave numbers in the fluid and the porous medium respectively, W and W_m are the velocities of the fluid and the porous layers in the vertical direction, $R_I=\frac{Qd^2}{\kappa}$ and $R_{I_m}=\frac{Q_m d_m^2}{\kappa_m}$ are the internal Rayleigh numbers of the fluid and porous layers $\tau_f=\frac{\kappa_{cf}}{\kappa}$ and $\tau_{mp}=\frac{\kappa_{cm}}{\kappa_m}$ are the solute to thermal diffusivity ratios in the fluid and porous layers respectively.

The corresponding boundary conditions for solving equations (15) to (20) (nondimesionalized and subjected to normal mode expansion) follows from Manjunatha and Sumithra (2018):

$$D^2W(1)+M_Ta^2\Theta(1)+M_sa^2S(1)=0 \quad \text{... (21)}$$

The velocity boundary conditions are:

$$\left.\begin{array}{r} W(1)=0;W_m(-1)=0;W_m(0)=\frac{\epsilon_T}{\zeta}W(0);\\ \left(D_m^2+a_m^2\right)W_m(0)=\frac{\epsilon_T}{\zeta^3}\left(D^2+a^2\right)W(0);\left(D^3-3a^2D\right)W(0)=-\frac{\zeta^4}{\epsilon_T Da}D_mW_m(0)\end{array}\right\} \quad \text{... (22)}$$

Thermodynamic boundary conditions are:

$$\left.\begin{array}{r} D\Theta(1)=0=D_m\Theta_m(-1)=0 \quad \text{(Adiabatic-Adiabatic condition);}\\ \Theta(0)=\frac{\epsilon_T}{\zeta}\Theta_m(0);D\Theta(0)=D_m\Theta_m(0);\\ D_m\Theta_m(-1)=0=\Theta_m(-1) \quad \text{(Adiabatic-Isothermal condition)}\end{array}\right\} \quad \text{... (23)}$$

Boundary criteria for salinity are as follows:

$$\left. DS(1)=0; \quad D_mS_m(-1)=0; \quad S(0)=\frac{\epsilon_s}{\zeta}S_m(0); \quad DS(0)=D_mS_m(0)\right\} \quad \text{... (24)}$$

Here $\zeta=\frac{d}{d_m}$ is the depth ratio, $\epsilon_T=\frac{\kappa}{\kappa_m}$ is the thermal diffusivity ratio, $\epsilon_s=\frac{\kappa_{cf}}{\kappa_{cm}}$ is the solute diffusivity ratio, $\beta^2=\frac{K}{d_m^2}=Da$ is the Darcy number, $M_s=-\frac{\partial\sigma}{\partial t}\frac{\left(T_0-T_u\right)d}{\mu\kappa}$ is the thermal Marangoni number and $M_s=-\frac{\partial\sigma}{\partial t}\frac{\left(c_0-c_u\right)d}{\mu\kappa}$ is the solute Marangoni number, where σ is the surface tension.

3. Solution by Exact method

For the above boundary conditions, thermal Marangoni number (Tmn) is obtained by using exact method for two different thermal boundary conditions viz; (i) both the upper surface of the fluid layer and the lower surface of the porous layer are adiabtic, and (ii) the upper surface of the fluid layer is adiabatic but the lower surface of the porous layer is isothermal.

The solutions for vertical velocities are obtained by solving equations (15) and (16) using velocity boundary conditions (22) and are as follows:

$$W(z) = (coshaz + A_{23}sinhaz + A_{33}zcoshaz + A_{43}zsinhaz)A_1 \quad \text{... (25)}$$

$$W_m(z_m) = \left(A_{m_{31}}cosha_m z_m + A_{m_{32}}sinha_m z_m\right)A_1 \quad \text{... (26)}$$

where $A_{m_{31}} = \frac{\epsilon_T}{\zeta}$; $A_{m_{32}} = \frac{\epsilon_T cosha_m}{\zeta sinha_m}$; $A_{23} = \frac{a_m \zeta^3 cosha_m}{2a^3(Da)sinha_m}$;

$A_{43} = \frac{a_m^2\zeta^2}{a} - a$; $A_{33} = \frac{-cosha-(A_{23}+A_{43})sinha}{cosha}$

The solutions for $S(z)$ and $S_m(z_m)$ are obtained by substituting $W(z)$ and $W_m(z_m)$ in equations (19) and (20) and using salinity boundary conditions (24).

$$S(z) = A_1\left(A_{53}coshaz + A_{63}sinhaz - \frac{1}{\tau_f}g_{r1}(z)\right) \quad \text{... (27)}$$

$$S_m(z_m) = A_1\left(A_{m_{33}}cosha_m z_m + A_{m_{34}}sinha_m z_m - \frac{1}{\tau_{mp}}g_{r2}(z_m)\right) \quad \text{... (28)}$$

where $g_{r1}(z) = g_1 + \frac{A_{33}}{4a}g_2 + \frac{A_{43}}{4a}g_3$, $g_1 = \frac{z}{2a}sinhaz + \frac{A_{23}z}{2a}coshaz$, $A_{53} = \delta_2 + \frac{\epsilon_s}{\zeta}A_{m_{33}}$

$g_2 = z^2 sinhaz - \frac{z}{a}coshaz + \frac{1}{2a^2}sinhaz$, $g_3 = z^2 coshaz - \frac{z}{a}sinhaz + \frac{1}{2a^2}coshaz$

$g_{r2}(z_m) = \frac{z_m A_{m_{31}}}{2a_m}sinha_m z_m + \frac{z_m A_{m_{32}}}{2a_m}cosha_m z_m$, $A_{63} = \frac{1}{a}\left(\delta_3 + a_m A_{m_{34}}\right)$, $\delta_2 = \frac{1}{8a^3\tau_f}\left\{\frac{a_m^2\zeta^2}{a} - a\right\}$

$A_{m_{33}} = \frac{acosha_m(\delta_1-\delta_2 sinha)-cosha(\delta_3 cosha_m+\delta_4 a_m)}{a_m(cosha)sinha_m+\frac{\epsilon_s}{\zeta}a(sinha)cosha_m}$, $A_{m_{34}} = secha_m\left(\delta_4 + A_{m_{33}}sinha_m\right)$,

$\delta_4 = \frac{1}{2a_m^2\tau_{mp}}\left[A_{m_{32}}(cosha_m + a_m sinha_m) - A_{m_{31}}(sinha_m + a_m cosha_m)\right]$

$\delta_1 = \frac{1}{a\tau}\left(\delta_{11} + \frac{A_{23}}{2}\delta_{12} + \frac{A_{33}}{4a}\delta_{13} + \frac{A_{43}}{4a}\delta_{14}\right)$, $\delta_3 = \frac{1}{\tau_f}\left\{\frac{A_{23}}{2a} - \frac{A_{33}}{4a^2}\right\} - \frac{A_{m_{32}}}{2a_m\tau_{mp}}$, $\delta_{14} = \frac{A_{43}}{4a}\left[cosha + \left(a - \frac{1}{a}\right)sinha\right]$

$\delta_{11} = \frac{1}{2a}(acosha + sinha)$, $\delta_{12} = \frac{A_{23}}{2a}(asinha + cosha)$, $\delta_{13} = \frac{A_{33}}{4a}\left[sinha + \left(a - \frac{1}{a}\right)cosha\right]$

3.1. To obtain Tmn M_{T_1} when the free surface and the rigid surface are both adiabatic (A-A)

The equations (17) and (18) are solved using (25), (26) and adiabatic boundary conditions as mentioned in (23) to obtain $\Theta_1(z)$ and $\Theta_{m1}(z_m)$.

$$\Theta_1(z) = A_1[c_{13}\cosh(bz) + c_{23}\sinh(bz) - f_1(z)] \quad \text{... (29)}$$

$$\Theta_{m1}(z_m) = A_1[c_{33}\cosh(b_m z_m) + c_{43}\sinh(b_m z_m) - f_{m1}(z_m)] \quad \text{... (30)}$$

The Tmn M_{T_1} obtained from the boundary condition (21) for the A-A case is:

where $b = \sqrt{a^2 - R_I}$ and $b_m = \sqrt{a_m^2 - R_{I_m}}$, $c_{13} = \Delta_1 + \frac{\epsilon_T}{\zeta}c_{33}$, $c_{23} = \frac{\Delta_3 - c_{13}b\sinh(b)}{b\cosh(b)}$

$c_{43} = \frac{c_{33}b_m\sinh(b_m)}{b_m\cosh(b_m)}$, $\Delta_1 = \left(\frac{A_{43}}{2a\sqrt{R_I}\sin(\sqrt{R_I})}\right)$, $\Delta_2 = \left(\frac{\sqrt{R_I}}{2a\sin(\sqrt{R_I})}\right)\left(A_{23} - \frac{A_{33}}{a} + \frac{aA_{33}}{R_I}\right) - \left(\frac{A_{m_{32}}\sqrt{R_{I_m}}}{2a_m\sin(\sqrt{R_{I_m}})}\right)$,

$c_{33} = \frac{-b\Delta_1\sinh(b)\cosh(b_m) - \Delta_2\cosh(b)\cosh(b_m) + \Delta_3\cosh(b_m) + \Delta_4\cosh(b)}{b_m\sinh(b_m)\cosh(b) + \frac{\epsilon_T}{\zeta}b\sinh(b)cosh(b_m)}$, $f_1(z) = \frac{1}{2asin\sqrt{R_I}}(f_{11} + f_{12} + f_{13})$

$\Delta_3 = \frac{1}{2a\sin(\sqrt{R_I})}(\eta_1 + A_{23}\eta_2 + A_{33}\eta_3 + A_{43}\eta_4)$, $f_{11} = (sinhaz + A_{23}coshaz)sin\left(\sqrt{R_I}z\right)$

$\eta_1 = a\cosh(a)\sin(\sqrt{R_I}) + \sqrt{R_I}\sinh(a)\cos(\sqrt{R_I})$, $f_{m1}(z_m) = \frac{sin\left(\sqrt{R_{I_m}}z_m\right)}{2a_m sin\sqrt{R_{I_m}}}\left(f_{m_{11}} + f_{m_{12}}\right)$

$$\eta_2 = a\sinh(a)\sin(\sqrt{R_I}) + \sqrt{R_I}\cosh(a)\cos(\sqrt{R_I}), \quad \Delta_4 = \frac{1}{2a_m\sin(\sqrt{R_{I_m}})}\left(A_{m_{31}}\Lambda_1 - A_{m_{32}}\Lambda_2\right)$$

$$\eta_3 = a\sin(\sqrt{R_I})\cosh(a) + \sqrt{R_I}\cosh(a)\cos(\sqrt{R_I}) - \tfrac{1}{a}\sqrt{R_I}\cos(\sqrt{R_I})\cosh(a)$$
$$- \sin(\sqrt{R_I})\sinh(a) + \tfrac{a}{\sqrt{R_I}}\cos(\sqrt{R_I})\cosh(a), \quad f_{m_{11}} = A_{m_{31}} sinha_m z_m$$

$$\eta_{41} = a\sin(\sqrt{R_I})\sinh(a) + \sqrt{R_I}\cos(\sqrt{R_I})\cosh(a) - \sin(\sqrt{R_I})\cosh(a)$$

$$f_{12} = A_{33}\left[\tfrac{1}{\sqrt{R_I}}(sinhaz)cos\left(\sqrt{R_I}z\right) + \left(zsinhaz - \tfrac{coshaz}{a}\right)sin\left(\sqrt{R_I}z\right)\right], \quad \eta_4 = \eta_{41} + \eta_{42}$$

$$f_{13} = A_{43}\left[\tfrac{1}{\sqrt{R_I}}(coshaz)cos\left(\sqrt{R_I}z\right) + \left(zcoshaz - \tfrac{sinhaz}{a}\right)sin\left(\sqrt{R_I}z\right)\right]$$

$$\Lambda_1 = a_m\cosh(a_m)\sin(\sqrt{R_{I_m}}) + \sqrt{R_{I_m}}\sinh(a_m)\cos(\sqrt{R_{I_m}}), \quad f_{m_{32}} = A_{m_{32}} cosha_m z_m$$

$$\Lambda_2 = a_m\sinh(a_m)\sin(\sqrt{R_{I_m}}) + \sqrt{R_{I_m}}\cos(\sqrt{R_{I_m}})\cosh(a_m), \ \eta_{42} = \left(\tfrac{a}{\sqrt{R_I}} - \tfrac{\sqrt{R_I}}{a}\right)\cos(\sqrt{R_I})\sinh(a)$$

$$M_{T_1} = -\frac{D^2W(1) + M_s a^2 S(1)}{a^2\Theta_1(1)} = -\frac{M_1 + M_s a^2\left(M_3 - \frac{1}{\tau_f}M_4\right)}{a^2(M_{21} - M_{22})}$$

where $M_1 = \left[a^2(1 + A_{33}) + 2aA_{43}\right]cosha + \left[a^2(1 + A_{43}) + 2aA_{33}\right]sinha$

$M_{21} = c_{13}coshb + c_{23}sinhb; \quad M_{22} = \frac{1}{2asin\sqrt{R_I}}(M_{23} + M_{24}A_{33} + M_{25}A_{43})$

$M_{23} = (sinha + A_{23}cosha)sin\sqrt{R_I}; \quad M_{24} = \left[sinha - \frac{cosha}{a}\right] + \frac{cos\sqrt{R_I}sinha}{\sqrt{R_I}}$

$M_{25} = \left[cosha - \frac{sinha}{a}\right]sin\sqrt{R_I} + \frac{cos\sqrt{R_I}cosha}{\sqrt{R_I}}; \quad M_3 = A_{53}cosha + A_{63}sinha$

$M_4 = \frac{sinha}{2a} + \frac{A_{23}cosha}{2a} + \frac{A_{33}}{4a}\left\{\left(1 + \frac{1}{2a^2}\right)sinha - \frac{cosha}{a}\right\} + \frac{A_{43}}{4a}\left\{\left(1 + \frac{1}{2a^2}\right)cosha - \frac{sinha}{a}\right\}$

3.2. To obtain Tmn M_{T_2} when the free surface is adiabatic and the rigid surface is isothermal (A-I)

The equations (17) and (18) are solved using $W(z)$, $W_m(z_m)$ and adiabatic-isothermal boundary conditions as mentioned in (23) to obtain $\Theta_2(z)$ and $\Theta_{m2}(z_m)$.

$$\Theta_2(z) = A_1\left[c_{12}coshbz + c_{22}sinhbz - f_2(z)\right] \quad \text{... (31)}$$

$$\Theta_{m2}(z_m) = A_1\left[c_{32}cosh(b_m z_m) + c_{42}sinh(b_m z_m) - f_{m2}(z_m)\right] \quad \text{... (32)}$$

where $b = \sqrt{a^2 - R_I}, \quad b_m = \sqrt{a_m^2 - R_{I_m}}, \quad c_{32} = \frac{1}{coshb_m}(\Upsilon_4 + c_{42}sinhb_m)$

$c_{42} = \frac{(\Upsilon_1 - \Upsilon_3 coshb)coshb_m - \left(\Upsilon_2 coshb_m + \Upsilon_4\frac{\epsilon_T}{\zeta}\right)bsinhb}{b\frac{\epsilon_T}{\zeta}(sinhb)sinhb_m + b_m(coshb)coshb_m}, \quad c_{22} = \frac{\Upsilon_3}{b} + \frac{b_m}{b}c_4, \quad c_{12} = \frac{\epsilon_T}{\zeta}c_{32} + \Upsilon_2$

$f_2(z) = f_1(z), \quad f_{m2}(z_m) = f_{m1}(z_m), \quad \Upsilon_4 = \frac{1}{2a_m}\left[A_{m_{31}}sinha_m - A_{m_{32}}cosha_m\right]$

$\Upsilon_3 = \Delta_2, \quad \Upsilon_2 = \Delta_1, \quad \Upsilon_1 = \Delta_3$

The Tmn M_{T_2} obtained from the boundary condition (21) for the A-I case is:

$$M_{T_2} = -\frac{D^2W(1) + M_s a^2 S(1)}{a^2\Theta_2(1)} = -\frac{M_2 + M_s a^2\left(M_3 - \frac{1}{\tau_f}M_4\right)}{a^2(M_{31} - M_{32})}$$

where $M_2 = M_1, \quad M_{31} = c_{12}coshb + c_{22}sinhb, \quad M_{32} = \frac{1}{2asin\sqrt{R_I}}(M_{33} + A_{33}M_{34} + A_{43}M_{35})$

$M_{33} = (sinha + A_{23}cosha)sin\sqrt{R_I}, \quad M_{34} = \left(sinha - \frac{cosha}{a}\right)sin\sqrt{R_I} + \frac{(sinha)cos\sqrt{R_I}}{\sqrt{R_I}}$

$M_{35} = \left(cosha - \frac{sinha}{a}\right)sin\sqrt{R_I} + \frac{(cosha)cos\sqrt{R_I}}{\sqrt{R_I}}$

4.0 Result and discussion

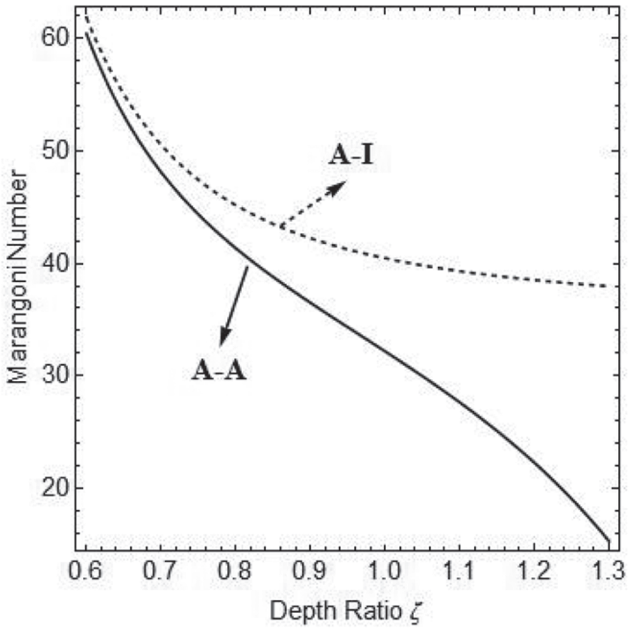

Figure 1: Comparison of M_{T1} and M_{T2}

Surface tension driven double diffusive convection (STDDDC) in a two-layer composite system with variable heat sources is compared for two thermal boundary conditions in this work: (i) A-A and (ii) A-I boundary conditions. The eigen value, Tmn is obtained using exact method for both the temperature boundary conditions. Below are graphical representations of Tmn for STDDDC as a function of physical parameters versus depth ratio ζ.

The comparison of M_{T1} , Tmn for adiabatic-adiabatic (A-A) condition and M_{T2} , Tmn for adiabatic-isothermal (A-I) condition is illustrated in figure 1. It is seen that M_{T2} is greater than M_{T1} , indicating that the A-I case is more stable than the A-A case for increasing depth ratio values, indicating that the fluid layer dominates the composite layer. Also, when the depth ratio increases, the Tmns decrease.

The graphs of Tmn's M_{T1} and M_{T2} for varying porous internal Rayleigh number R_{Im} = 0.2, 0.5, 1 and fixed parameters Da = 0.005, R_I = 1, a = 1.3, $\varepsilon_s = \varepsilon_T$ = 0.5, $\tau_f = \tau_{mp} = M_s$ = 1 are shown in figures 2(a) and 2(b) respectively. For the A-A and A-I cases, the Tmn's, M_{T1} and M_{T2} decrease with increas- ing values of R_{Im}. As a result, increasing this parameter's value causes the system to destabilize. The curves diverge, showing that the effect of this parameter is more pronounced for higher depth ratio values, i.e. for fluid layer dominated composite systems.

In figure 3, the effects of fluid internal Rayleigh number for R_I = 0.2, 0.5, 1 and a = 1.3, Da = 0.005, $\varepsilon_s = \varepsilon_T$ = 0.5, $R_{Im} = \tau_f = \tau_{mp} = M_s$ = 1 is shown. The Tmn's, M_{T1} and M_{T2} are showing decreasing effect when R_I is increasing which indicates that the system is

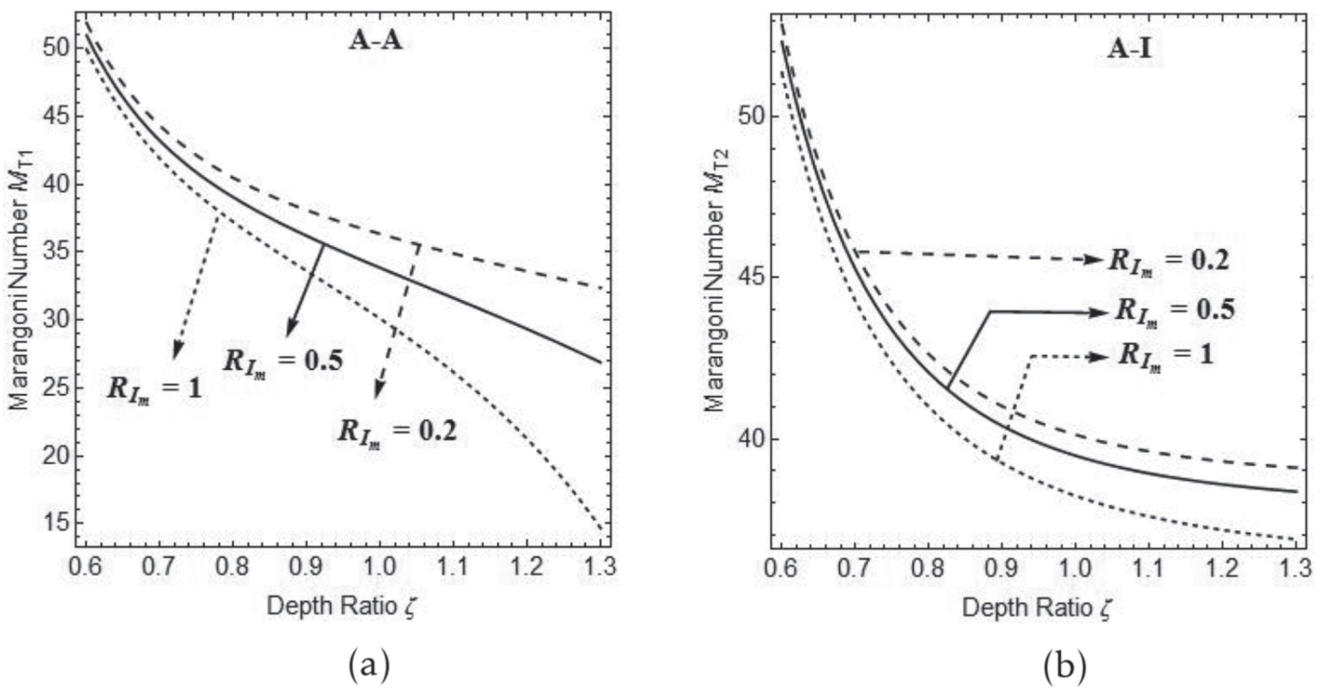

Figure 2: Effects of R_{Im}

destabilized and so the onset of STDDDC convection occurs faster. The curves for increasing depth ratios diverge for both the A-A and A-I cases, demonstrating that this parameter is important for fluid layer dominating composite systems.

The variations of solute diffusivity ratio ε_s = 0.1, 0.5, 1 are shown in figure 4 while other physical parameters a = 1.3, Da = 0.005, ε_T = 0.5, $R_I = R_{Im} = \tau_f = \tau_{mp} = M_s = 1$ are fixed. For larger values of depth ratio, the curves of M_{T_1} and M_{T_2} converge, indicating that this parameter is effective for porous dominant composite systems. As Es increases, M_{T_1} and M_{T_2} decreases, the

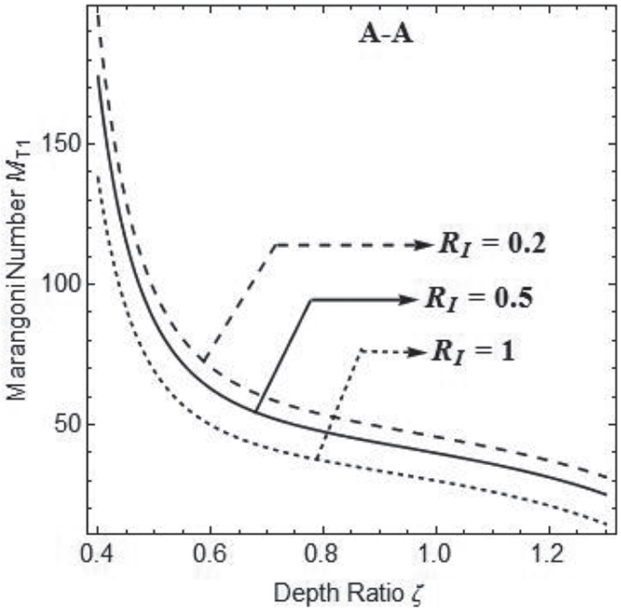

(a)

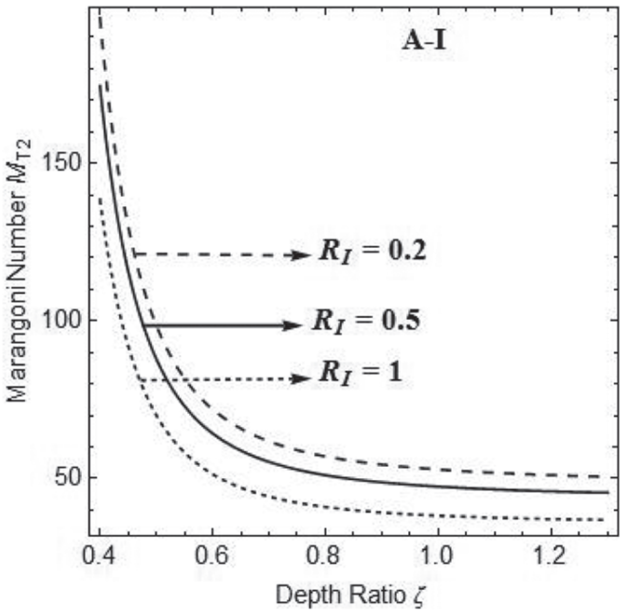

(b)

Figure 3: Effects of R_I

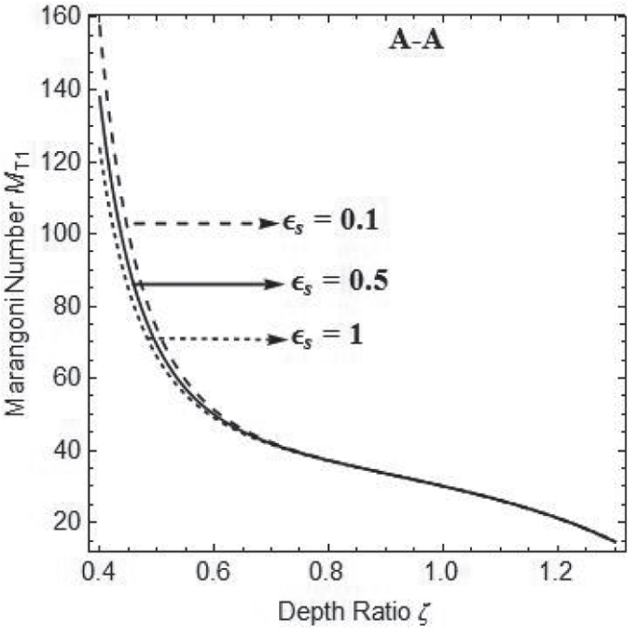

(a)

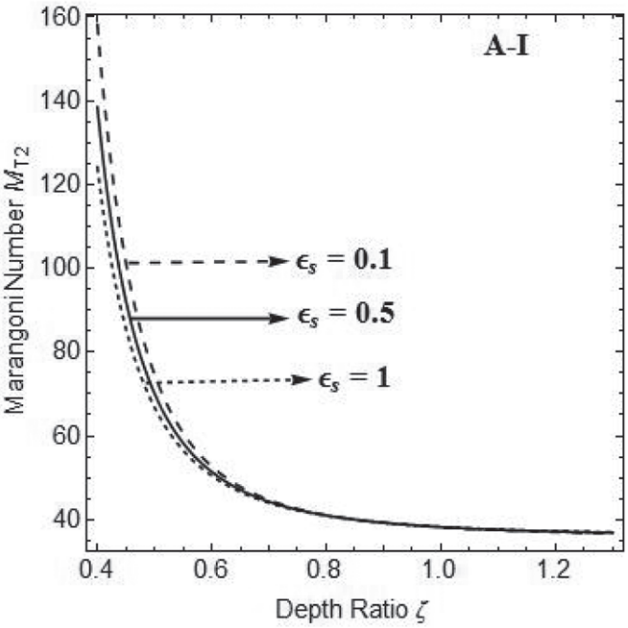

(b)

Figure 4: Effects of ε_s

system is destabilized and hastening the onset of STDDDC.

In figures 5(a) and 5(b) the effects of thermal diffusivity ratio $\varepsilon_T = 0.1, 0.5, 1$ on Tmn's for $a = 1.3$, $Da = 0.005$, $\varepsilon_s = 0.5$, $R_I = R_{Im} = \tau_f = \tau_{mp} = M_s = 1$ are shown. Increasing the values of ε_T, M_{T1} and M_{T2} increases for $\zeta < 0.5$ and decreases for $\zeta > 0.5$. The range of depth ratio plays a significant role. Thus, the onset of STDDDC can be postponed or preponed by choosing suitable range of depth ratio and thermal diffusivity ratio.

The effects of Darcy number $Da = 0.01, 0.005, 0.0001$ for fixed parameters $a = 1.3$, $R_I = R_{Im} = \tau_f = \tau_{mp} = M_s = 1$,

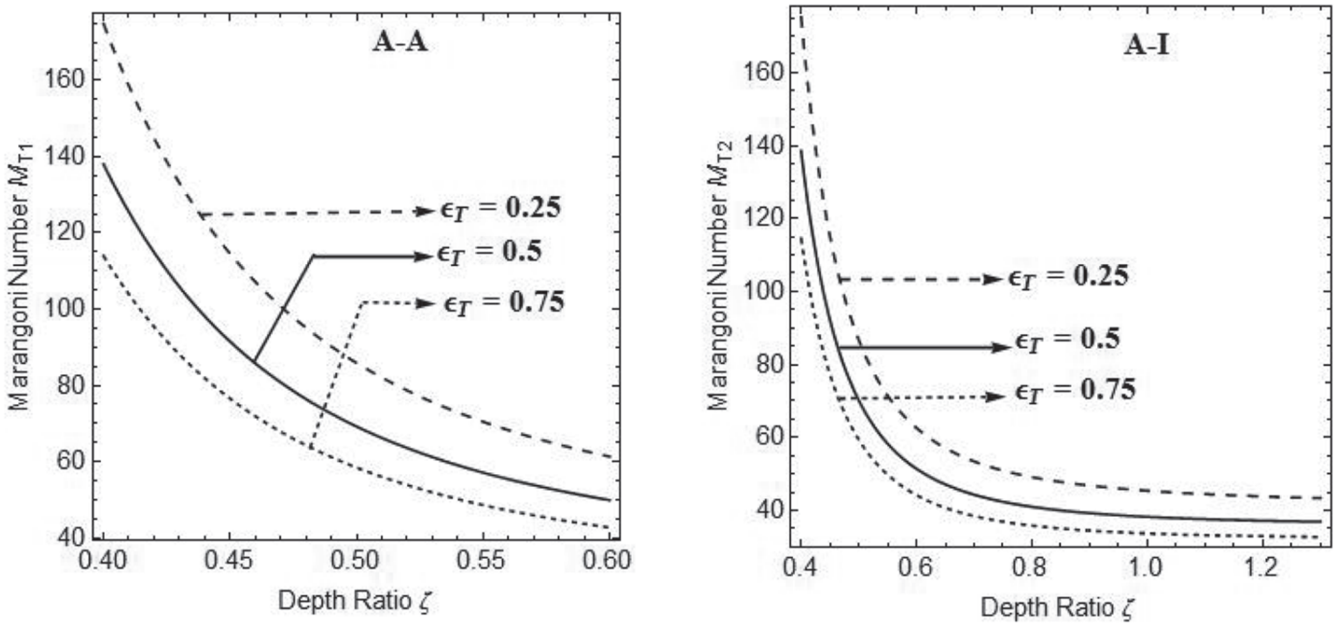

(a) (b)

Figure 5: Effects of ε_T

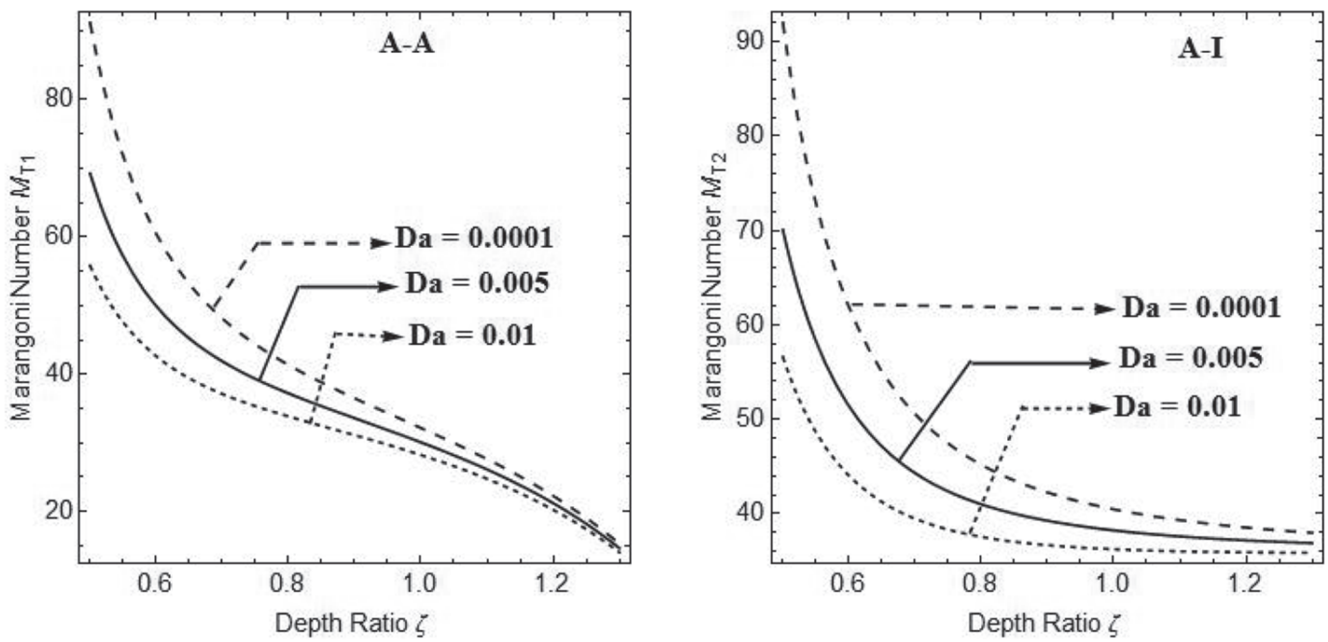

(a) (b)

Figure 6: Effects of *Da*

$\varepsilon_s = \varepsilon_T = 0.5$ are depicted in figure 6. As Darcy number increases, M_{T_1} and M_{T_2} decreases thus the onset of STDDDC is enhanced by stabilizing the system. Also, the curves in figures 6(a) and 6(b) are widely diverging for lower depth ratio values $\zeta = \frac{d}{d_m}$. This shows that the Darcy number is crucial in the porous layer dominated composite system.

Figure 7 exhibits the effect of $a = 1.2, 1.3, 1.45$ on Tmn's M_{T_1} and M_{T_2} for the fixed parameters $\varepsilon_T = \varepsilon_s = 0.5$, $Da = 0.005$, $R_I = R_{Im} = \tau_f = \tau_{mp} = M_s = 1$. Figures 7(a) and 7(b) show that as a increases, M_{T_1} and M_{T_2} increases as well, indicating that the system has stabilizing effect.

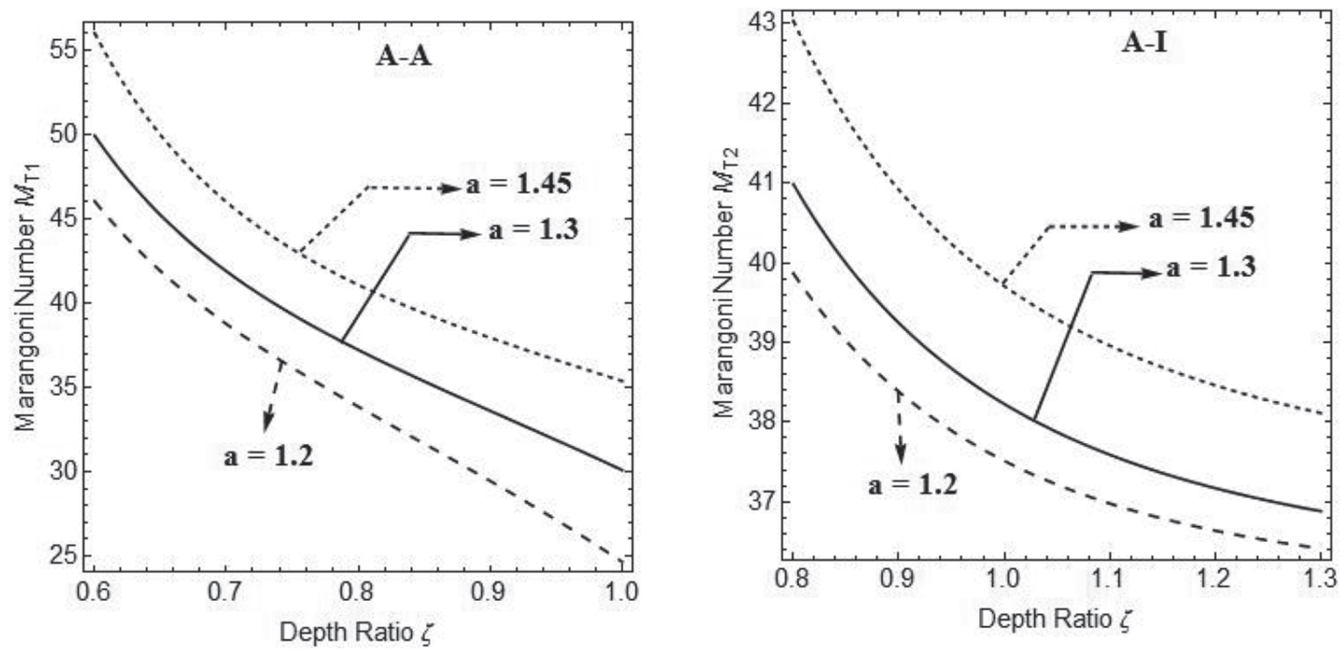

(a)

Figure 7: Effects of *a*

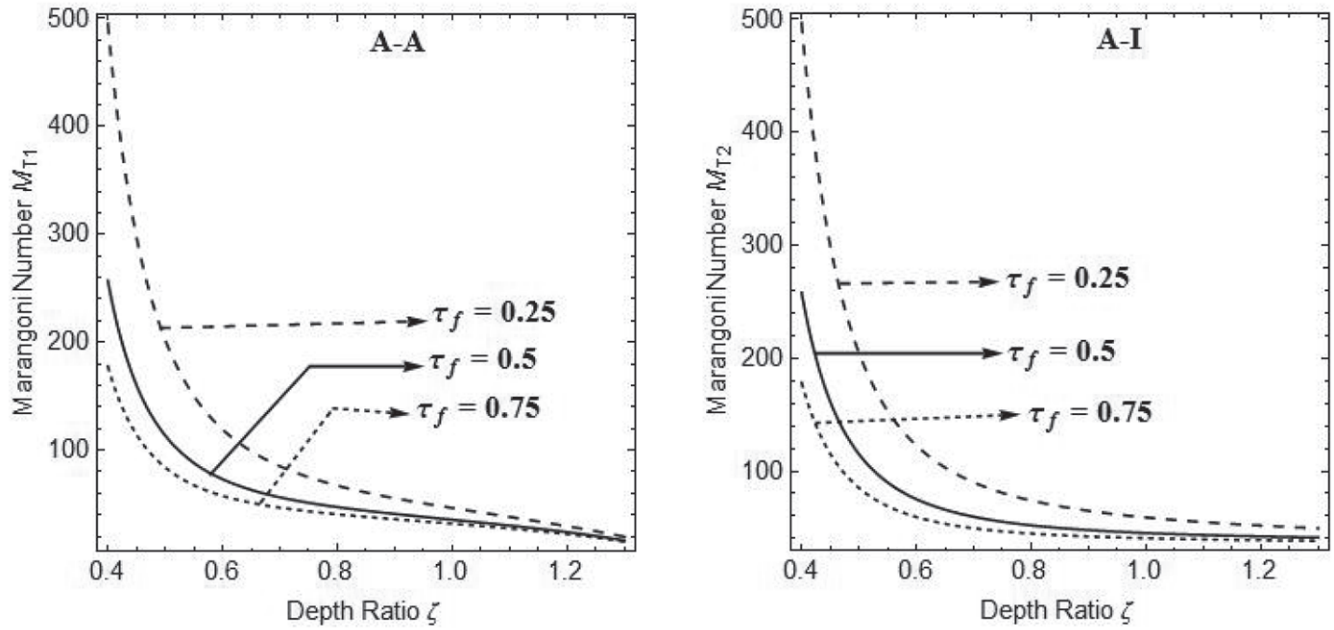

(a) (b)

Figure 8: Effects of τ_f

In figures 8(a) and 8(b) we can see the variations of diffusivity ratio $\tau_f = 0.25, 0.5, 0.75$, the solute to thermal diffusivity ratio in the fluid layer. The Tmn's M_{T_1} and M_{T_2} decreases for increase in τ_f, thus destabilizing the system. Furthermore, the variations of τ_f are noticed only for smaller ζ values, i.e. for porous dominated composite systems.

Figures 9(a) and 9(b) show the impacts of τ_{mp}, which is the ratio of solute to thermal diffusivity of the porous layer. As the depth ratio increases, the curves decline in the case of A-A, increase in the case of A-I, and converge at larger depth ratios. Both M_{T_1} and M_{T_2}

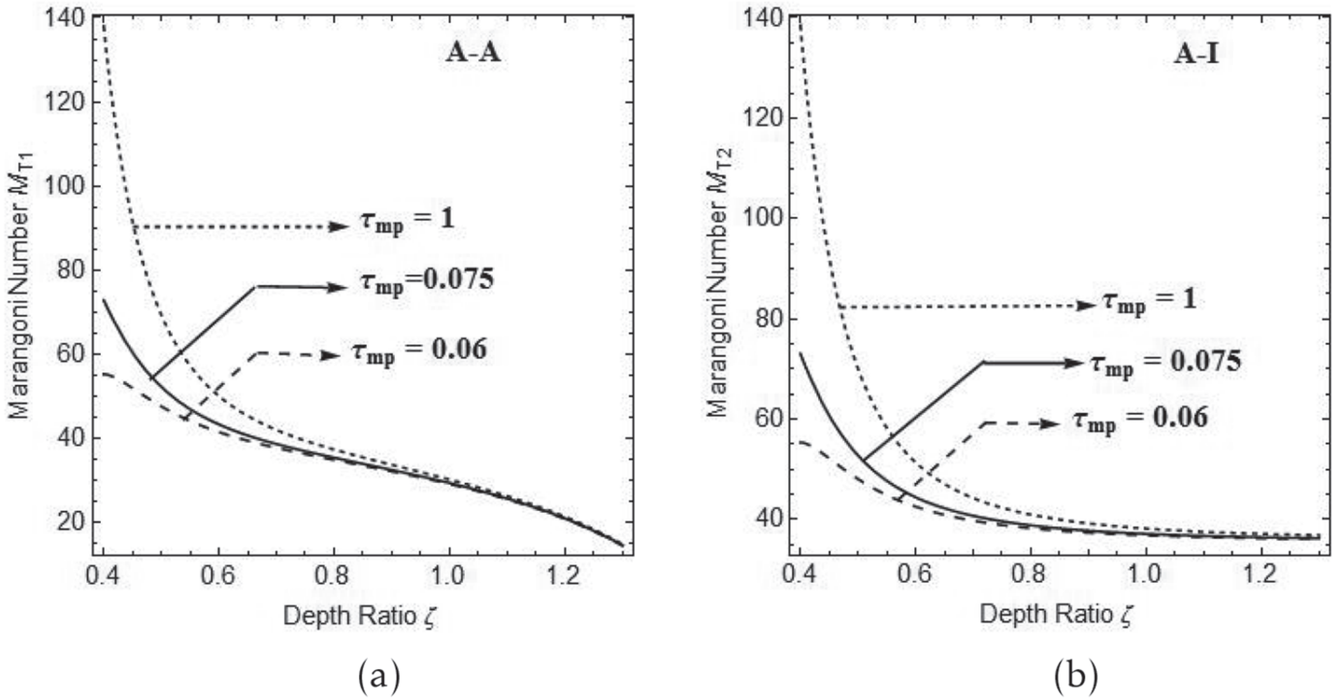

Figure 9: Effects of τ_{mp}

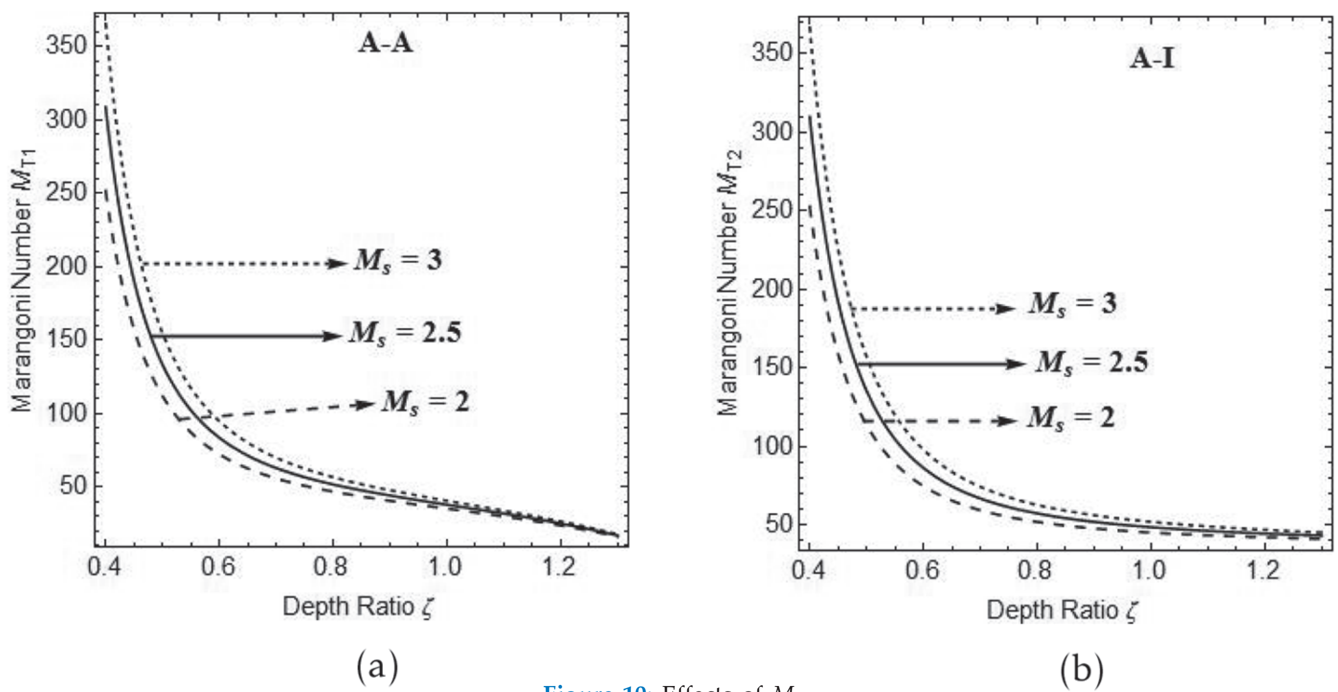

Figure 10: Effects of M_s

decreases with increase in τ_{mp} which destabilizes the system so that STDDDC sets in faster.

Figures 10(a) and 10(b) depicts the variations of solute Marangoni number M_s = 2, 2.5, 3 with respect to depth ratio for a = 1.3, Da = 0.005, $\varepsilon_T = \varepsilon_s$ = 0.5, $R_I = R_{Im} = \tau_f = \tau_{mp}$ = 1. The Tmn's M_{T1} and M_{T2} increases as M_s increases, indicating that there is a stabilising influence on the system, delaying the onset of STDDDC.

5. Conclusions

The effects of two temperature boundary conditions, (i) A-A and (ii) A-I, on STDDDC for variable heat sources, are investigated in this study. The findings reveal that:

1. When compared to both insulating surfaces, the system is more stable for lower isothermal and upper adiabatic surfaces.
2. For both temperature boundary conditions, larger internal Rayleigh numbers in both fluid and porous layers, as well as the solute diffusivity ratio, have a destabilising effect, hastening the onset of STDDD convection.
3. For both A-A and A-I situations, higher values of the solute Marangoni number, Darcy number, and thermal diffusivity ratio have a stabilising effect, delaying the onset of STDDDC.

Acknowlodgements

The first author, Sumithra. R expresses her heartfelt gratitude to VGST, KSTeps Bengaluru, Karnataka, India for sponsoring this investigation under K-FIST L2 Scheme.

References

[1] Altawallbeh, A.A., Bhadauria, B.S., and Hashim, I. Linear and nonlinear double-diffusive convection in a saturated anisotropic porous layer with soret effect and internal heat source. International Journal of Heat and Mass Transfer, 59(2013), 103-111.

[2] Bahadori, F and Rezvantalab, S. Effects of temperature and concentration dependent viscosity on onset of convection in orous media. Journal of Chemical Technology and Metallurgy, 49(2014), 541-544.

[3] Bergman, T.L. Numerical simulation of double-diffusive Marangoni convection. Physics of Fluids, 29(1986), 2103-08.

[4] Gaikwad, S.N., and Dhanraj, M. Onset of double diffusive reaction-convection in an anisotropic porous layer with internal heat source. 5th International Conference on Porous Media and Their Applications in Science, Engineering and Industry, ECI Symposium Series(2104).

[5] Gangadharaiah, Y.H. Double diffusive surface yension driven convection in a superposed fluid-porous system. internationl Journal of Thermofluid Science and Technology, 8(2021), 080301.

[6] Hill, A.A. Double-diffusive convection in a porous medium with a concentration based internal heat source. Proc. Roy.Soc.A, 461(2005), 56-574.

[7] Khalid, I.K., Mokhtar, N.F.M., Hashim, I., Ibrahim, Z.B., Gani, S.S.A. Effect of internal heat source on the onset of double-diffusive convection in a rotating nanofluid layer with feedback control strategy. Advances in Mathematical Physics, 2017(2017), 1-12.

[8] Manjunatha, N and Sumithra, R. Effects of non-uniform temperature gradients on double diffusive Marangoni convection in a two layer system. International Journal of Pure and Aplied Mathematics, 118(2018), 203-219.

[9] Majunatha, N., Sumithra, R., Vanishree, R.K. Darcy-Benard double diffusive Marangoni convection in a composite system with constant heat source along with non uniform temperature gradients. Malayasian Journal of Fundamental and Applied Sciences, 17(2021), 7-15.

[10] Ming-I Char and Ko-Tai Chang. Effect of interfacial deformation on the onset of convective instability in a doubly diffusive fluid layer. International Journal of Heat and Mass Transfer, 39(1996), 407-418.

[11] Neela, Deepika and Matta, Anjanna and Anantha, Lakshmi Narayana, Puranam. Effect of throughflow on double diffusive convection in a porous medium with concentration based internal heat source. Journal of Porous Media, 19(2016), 303-312.

[12] Sumithra, R. Mathematical modeling of Hydrothermal growth of crystals as double diffusive convection in composite layer bounded by rigid walls. International Journal of Engineering Sci- ence and Technology, 4(2012), 779-791.

[13] Sumithra, R., Archana, M.A., Vanishree, R.K. Darcy-Benard surface tension driven convection in a composite layer with temperature dependent heat source. Malaya Journal of Mathematik, 8(2020), 2074-81.

[14] Sumithra, R., Vanishree, R.K., Deepa R Acharya. Non-Darcian Benard Marangoni Convection in a superposed fluid-porous layer with temperature dependent heat source. Malaya Journal of Mathematik, 8(2020), 2233-42.